Vibronic intensities in the absorption spectra of Yb^{3+}

R. Acevedo
Department of Basic Chemistry, Faculty of Physical and Mathematical Sciences, University of Chile, Tupper 2069, P.O. Box 2777, Santiago, Chile

P. A. Tanner
Department of Biology and Chemistry, City University of Hong Kong, Tat Chee Avenue, Kowloon, Hong Kong

T. Meruane
Department of Chemistry, Metropolitan University of Educational Sciences, Av. J. P. Alessandri 774, P.O. Box 147-C, Santiago, Chile

V. Poblete
Department of Basic Chemistry, Faculty of Physical and Mathematical Sciences, University of Chile, Tupper 2069, P.O. Box 2777, Santiago, Chile

(Received 23 October 1995)

The oscillator strengths and relative vibronic intensity distribution of the $(^2F_{5/2})\Gamma_8,\Gamma_7 \leftarrow \Gamma_6(^2F_{7/2})$ transitions of the $YbCl_6^{3-}$ complex ion at an octahedral symmetry site in the $Cs_2NaYbCl_6$ lattice have been measured experimentally and calculated using a combined vibronic crystal-field–ligand polarization approach. The vibronic crystal-field contribution to the total transition dipole moment of the various excitations was worked out both with and without invoking closure over the central metal ion intermediate electronic states and the intensity was assumed to be derived from both a parity and a spin-allowed $d \leftarrow f$ transition with the cooperation of the odd-parity vibrational modes of the complex ion. Quadrupole and hexadecapole terms have been included in the ligand polarization contribution. Attention has been given to the correct choice of phases for both the electronic and the vibrational wave functions in order to ensure the right sign for the cross term which couples together the crystal field and the ligand polarization transition dipole vectors. The *ab initio* formalism employed avoids the use of any adjustable parameters in calculating the vibronic intensities. The calculated oscillator strengths of vibronic transitions are within order of magnitude agreement with experimental values. The sensitivity of the calculated values to the use of different force fields has been investigated. The experimentally measured total oscillator strengths for the $(^2F_{5/2})\Gamma_8,\Gamma_7 \leftarrow \Gamma_6(^2F_{7/2})$ transitions of $YbCl_6^{3-}$ diluted into the transparent $Cs_2NaGdCl_6$ host remain constant with change in Yb^{3+} concentration although deviation of the chromophore from octahedral symmetry is evident at intermediate concentrations. A comparison with the vibronic sidebands of $Cs_2LiYbCl_6$ and Cs_2KYbF_6 is made. [S0163-1829(96)05329-5]

I. INTRODUCTION

The electronic absorption, excitation, and emission spectra of the lanthanide hexachloroelpasolites of general formula Cs_2 $NaLnCl_6$ have been studied in detail in order to provide information about the crystal-field[1] (CF) and energy-transfer processes[2] occurring in these lattices. The electronic spectra of these solid-state compounds comprise zero-phonon lines (ZPL's) and broader structure due to vibronic origins in which one quantum of an odd vibrational mode of $LnCl_6^{3-}$, or a lattice mode, is excited. The first members of progressions in the totally symmetric lanthanide-chloride stretching mode upon these vibronic origins are very much weaker, since the bond length changes in the intraconfigurational transitions are small. The intensities of the ZPL enabled by the magnetic dipole[3] (MD) or electric quadrupole[4] (EQ) mechanisms are generally well accounted for by theory. The theoretical explanation of the striking changes in vibronic intensity from one electronic transition to another has been the subject of several papers and comprises the major part of the present study. The approach of Richardson and co-workers[5] was based upon numerical differentiation of both the CF and the ligand polarization (LP) geometric factors and was not intended to identify the separate contributions of the CF, LP and the interference terms which are scaled by ill-defined quantities. The CF contribution to the total transition dipole moment of the various excitations was calculated using the closure procedure over the lanthanide-ion intermediate states. Several problems associated with this approximation have been discussed in the context of the transition elements[6–8] and are likely to remain for lanthanide elements. The detailed studies of Richardson and the more recent refinements to this approach by Malta were also flawed by incorrect vibrational assignments[9] and a poor description of the vibrational force field.[10,11] Judd[12] has given an alternative treatment to that of Richardson but which apparently gave similar calculated results. The intensities of vibronic origins of UCl_6^{2-} have been parametrized, but the number of parameters employed for the vibronic intensity due to one (ν_3) mode of vibration has been formidable: 11 or 6 (Ref. 13) and 9.[14] Following these studies, there has been an upsurge of interest in vibronic intensities, but mainly from qualitative point of view.[15–17] Quantitative vibronic intensity calculations have been performed for complex ions of some

d-block elements[18,19] and a preliminary study has been made for the lanthanide complex ion $PrCl_6^{3-}$.[20] The present study extends the application of the model to the absorption spectra of Yb^{3+} and examines, using the vibronic oscillator strengths, the sensitivity of calculated values to the treatment of the vibrational data, and of measured values to chromophore concentration and host lattice. Data have been reported for the actinide system UCl_6^{2-},[13] but no vibronic oscillator strengths are available for an octahedral lanthanide complex ion for comparison with calculation. The theory of one-center vibronic transitions presented herein differs in several respects from that for two-center cooperative vibronic transitions[21,22] which have been investigated experimentally for the OH stretching vibration coupled to intraconfigurational f-f electron transitions.[23–25] In the two-center theory, the intensity of the vibronic transition is envisaged to arise from the dipole-dipole interaction between the f-electron transition to an odd-parity state and the oscillating vibration, and is thus related to the infrared absorption strength of the vibration. The concepts and similarities between the theories of Judd,[12] Richardson,[9,10] and Stavola[21,22] have been summarized elsewhere.[25,26]

The site symmetry of Ln=Gd and Yb in $Cs_2NaLnCl_6$ is taken to be octahedral in our model, which is in accordance with our 10-K Raman data for $Cs_2NaGd_xYb_{1-x}Cl_6$ ($x=0$ to 1), but the zero-phonon line splittings of several wave numbers observed in the $\Gamma_8 \leftarrow \Gamma_6$ 10-K absorption spectra for $Cs_2NaGd_xYb_{1-x}Cl_6$ ($x=0.1$–0.9) indicate a small distortion. Phase transitions have been observed at low temperatures for Ln=Ce, Pr, Nd but not for Ln=Ho, Tm, Yb in $Cs_2NaLnCl_6$, using neutron diffraction and solid-state NMR.[27–29] Raman spectra at 12 K show no deviation from octahedral symmetry for Yb^{3+} in $Cs_2NaYbCl_6$.[30] X-ray[29] and optical[31] measurements show that $Cs_2NaGdCl_6$ is cubic at 10 K.

The vibronic intensity model views the $LnCl_6^{3-}$ anions as isolated chromophores in the crystal lattice and considers the intensity arising only from $\mathbf{k}=0$ ungerade internal modes of vibration. The contributions to the vibronic intensity arise from the CF (static-coupling) and LP (dynamic coupling) mechanisms. By contrast to previous vibronic intensity models, our model employs no adjustable parameters, requiring only the empirical knowledge of the ligand subsystem effective charges and polarizability values, the metal-ligand bond distance, the energy gap corresponding to both a parity and spin-allowed transition, expectation values of r^k (such as $\langle r^k \rangle_{ff}$ and $\langle r^k \rangle_{fd}$) and the details of the assumed vibrational force field. The calculation is performed within the framework of the independent system model[32] (ISM) so that effects such as charge-transfer and other related phenomena[33] are excluded.

For comparison with the results from $Cs_2NaYbCl_6$, experimental vibronic intensity data have also been provided in this study for two other elpasolite systems: $Cs_2LiYbCl_6$ and Cs_2KYbF_6, both compounds being cubic at room temperature.[34] To our knowledge, there has not been a previous study of the absorption spectrum of a lanthanide hexafluoroelpasolite, although the magnetic behavior of Cs_2KYbF_6 (Ref. 35) and Cs_2NaYbF_6,[36,37] and the room-temperature Raman spectrum of Cs_2KYbF_6 (Ref. 38) have been reported.

II. EXPERIMENT

Hexachloroelpasolites were prepared according to Morss method *E* (Ref. 39) and the powders were dried in vacuo at 300 °C prior to sealing in quartz tubes and passing through a Bridgman furnace at 850 °C. Cs_2NaYbF_6 was prepared by heating the anhydrous fluorides (Strem Chemicals) in a platinum crucible, under a stream of nitrogen gas at 1100 °C. Absorption spectra were recorded using a Biorad FTS-60A spectrometer equipped with an Oxford Instruments closed-cycle cooler cryostat. Raman spectra were recorded using a Spex 1403-DM spectrometer. Both instruments were calibrated to vacuum wave numbers. Using polarized radiation, the oscillator strength, P_{if}, of a band in the absorption spectrum was calculated using the terminology in Ref. 40:

$$P_{if}=\frac{4m_e c\varepsilon_0}{Le^2}\ln 10\int \varepsilon(\nu)d\nu, \tag{1}$$

which, on rearrangement in terms of the lattice parameter of $Cs_2NaYbCl_6$, $a=1066.7\pm1.1$ pm,[34] crystal thickness, b/cm, and absorbance, $A(\overline{\nu})$ at wave number $\overline{\nu}$ becomes

$$P_{if}=6.5033\times10^{-19}a^3b^{-1}\int A(\overline{\nu})d\overline{\nu}. \tag{2}$$

The refractive index of crystals of $Cs_2NaYbCl_6$ was measured by immersion[41] from 450 to 700 nm and fitted to the formula

$$n=1.582\,681+125\,47\lambda^{-2}, \tag{3}$$

where λ is in nm.

III. METHOD OF CALCULATION

In the ISM the total transition dipole moment associated with the $\Gamma_2\gamma_2 \leftarrow \Gamma_1\gamma_1$ electronic transition (where Γ_i is the ith irrep, and γ_i the ith component of the ith irrep in the octahedral molecular point group) may be written as the sum of CF and LP contributions:[42]

$$\vec{\mu}_{\rm tot}(\Gamma_2\gamma_2\leftarrow\Gamma_1\gamma_1)=\vec{\mu}_{\rm CF}(\Gamma_2\gamma_2\leftarrow\Gamma_1\gamma_1)+\vec{\mu}_{\rm LP}(\Gamma_2\gamma_2\leftarrow\Gamma_1\gamma_1). \tag{4}$$

These two terms are considered in detail in the next two sections.

A. The crystal-field term

The θth component of the electronic factor associated with the CF contribution to the vibronic intensity induced by the tth odd-parity mode of vibration is written as

$$U_{\nu_t}^{\mathrm{CF},\theta}=\frac{1}{\Delta E}\sum_{\alpha\Gamma\gamma}\{\langle {}^2F_{7/2}\Gamma_6\gamma_6|\mu^\theta|\alpha\Gamma\gamma\rangle\langle\alpha\Gamma\gamma|V_{\nu_t}|{}^2F_{5/2}\Gamma_x\gamma_x\rangle+\langle {}^2F_{7/2}\Gamma_6\gamma_6|V_{\nu_t}|\alpha\Gamma\gamma\rangle\langle\alpha\Gamma\gamma|\mu^\theta|{}^2F_{5/2}\Gamma_x\gamma_x\rangle\},\tag{5}$$

where ${}^2F_{7/2}, {}^2F_{5/2}, \alpha$ stand for the *LSJ* parentage of the initial, terminal, and intermediate electronic states. For the $({}^2F_{5/2})\Gamma_8,\Gamma_7\leftarrow\Gamma_6({}^2F_{7/2})$ electronic transitions the summation is, in principle, over all intermediate states derived from the $f^{12}d$ and $f^{12}g$ configurations, but we restrict it to a single $f^{12}d$ state. μ^θ represents the θth component of the lanthanide-ion electric dipole, $\mu^\theta=-iM_\theta^{T_1}$, and the vibronic operators[43] are defined as

$$V_{\nu_t}=\sum_k A_{\nu_t}^{\Gamma\gamma}(k)M_\gamma^\Gamma(k),\tag{6}$$

that is, as products of the CF vibronic coupling constants, $A_{\nu_t}^{\Gamma\gamma}(k)$, and the symmetrized lanthanide-ion multipoles, $M_\gamma^\Gamma(k)$, the additional label k distinguishing the multipole rank. When considering the $\nu_3(\tau_{1u})$, $\nu_4(\tau_{1u})$, and $\nu_6(\tau_{2u})$ $LnCl_6^{3-}$ moeity modes, k may take the values 1, 3, and 5, but the last of these values is shown to make a negligible contribution and has been neglected in our calculations. The effective average energy, ΔE, in (5) corresponds to the energy gap between the $f^{12}d$ and f^{13} configurations.

A relevant vibronic matrix element in (5) is of the form

$$\langle\alpha_1\Gamma_1\gamma_1|M_\gamma^\Gamma(k)|\alpha_2\Gamma_2\gamma_2\rangle=(-1)^{\Gamma_1+\gamma_1^+}V\begin{pmatrix}\Gamma_1 & \Gamma_2 & \Gamma\\ \gamma_1^+ & \gamma_2 & \gamma\end{pmatrix}\langle\alpha_1\Gamma_1\|M_\gamma^\Gamma(k)\|\alpha_2\Gamma_2\rangle,\tag{7}$$

where the reduced matrix elements can be conveniently expressed in terms of the symmetry-adapted factors $Z_k^\Gamma(\Gamma_1J_1|\Gamma_2J_2)$ which are tabulated in Appendix A 2.

The relevant master equation is

$$\langle\alpha_1\Gamma_1\|M_\gamma^\Gamma(k)\|\alpha_2\Gamma_2\rangle=Z_k^\Gamma(\Gamma_1J_1|\Gamma_2J_2)\langle\alpha_1\|C^k\|\alpha_2\rangle.\tag{8}$$

Thus the θth component contributing to the electric dipole vibronic transition moments associated with the $({}^2F_{5/2})\Gamma_8,\Gamma_7\leftarrow\Gamma_6({}^2F_{7/2})$ excitations may be written as

$$\begin{aligned}\mu^{\mathrm{CF},\theta}({}^2F_{5/2}\Gamma_x\gamma_x\leftarrow\Gamma_6\gamma_6{}^2F_{7/2})=-\frac{Ze}{\Delta E}\sum_{kt}S_{kt}\sum_{\Gamma\gamma}\sum_{i\tau}A_{kt}^{\Gamma\gamma}(i,\tau)\sum_{\psi''}\{&\langle {}^2F_{7/2}\Gamma_6\gamma_6|M_\gamma^\Gamma(i,\tau)|\psi''\rangle\langle\psi''|\mu^\theta|{}^2F_{5/2}\Gamma_x\gamma_x\rangle\\&+\langle {}^2F_{7/2}\Gamma_6\gamma_6|\mu^\theta|\psi''\rangle\langle\psi''|M_\gamma^\Gamma(i,\tau)|{}^2F_{5/2}\Gamma_x\gamma_x\rangle\},\end{aligned}\tag{9}$$

with the intermediate states designated as $|\psi''\rangle=|[L''(1/2)J'']\Gamma''\gamma''\rangle$. The relevant nonzero products $\langle {}^2F_{7/2}\Gamma_6\gamma_6|M_\gamma^\Gamma(i,\tau)|\psi''\rangle\langle\psi''|\mu^\theta|{}^2F_{5/2}\Gamma_x\gamma_x\rangle$ and $\langle {}^2F_{7/2}\Gamma_6\gamma_6|\mu^\theta|\psi''\rangle\langle\psi''|M_\gamma^\Gamma(i,\tau)|{}^2F_{5/2}\Gamma_x\gamma_x\rangle$ are listed in Appendix A. On expansion of the symmetrized lanthanide-ion multipoles, $M_\gamma^\Gamma(i,\tau)$, and also of the θth component of the lanthanide-ion electric dipole, in terms of the Garstang tensor operators $D_q^k=-er^kC_q^k(\theta,\phi)$, the product matrix elements of the above equation are ultimately expressed as

$$\langle {}^2F_{7/2}\Gamma_6\|C^k\|L''\tfrac{1}{2}J''\rangle\langle L''\tfrac{1}{2}J''\|C^1\|{}^2F_{5/2}\rangle,$$

and also

$$\langle {}^2F_{7/2}\Gamma_6\|C^1\|L''\tfrac{1}{2}J''\rangle\langle L''\tfrac{1}{2}J''\|C^k\|{}^2F_{5/2}\rangle.$$

B. The ligand polarization term

The θth component of the LP contribution to the total transition dipole moment may be evaluated from the expression[42]

$$\mu^{\mathrm{LP},\theta}({}^2F_{5/2}\Gamma_x\gamma_x\leftarrow\Gamma_6\gamma_6{}^2F_{7/2})=\sum_{kt}S_{kt}\sum_{\Gamma\gamma}\sum_{i\tau}B_{kt}^{\Gamma\gamma\theta}(i,\tau)\langle {}^2F_{7/2}\Gamma_6\gamma_6|M_\gamma^\Gamma(i,\tau)|{}^2F_{5/2}\Gamma_x\gamma_x\rangle,\tag{10}$$

where

$$B_{kt}^{\Gamma\gamma\theta}(i,\tau) = -\alpha_L \sum_L \{\partial G_{\Gamma\gamma\theta}^{\mathrm{LP}}(i,\tau)/\partial S_{kt}\}_0 . \quad (11)$$

$G_{\Gamma\gamma\theta}^{\mathrm{LP}}(i,\tau)$ are the symmetry-adapted ligand polarization geometric factors which have been tabulated,[43] and S_{kt} are the symmetry coordinates of the complex ion (i.e., the linear combination of the nuclear Cartesian displacement coordinates). The quantities α_L are the mean polarizability of the chloride ligands, measured at the frequency of the electronic transition. In order to evaluate the matrix elements: $\langle {}^2F_{7/2}\Gamma_6\gamma_6|M_\gamma^\Gamma(i,\tau)|^2F_{5/2}\Gamma_x\gamma_x\rangle$ the symmetry-adapted central metal ion multipoles are expressed in terms of Racah tensor operators:

$$M_\gamma^\Gamma(i,\tau) = \sum_q R_{iq}^{\Gamma\gamma}(i,\tau) D_q^i(\theta,\phi), \quad (12)$$

where the expansion coefficients $R_{iq}^{\Gamma\gamma}(i,\tau)$ have been tabulated.[44,45] The relevant matrix elements are ultimately reduced to monoelectronic matrix elements of the form $\langle 3m|C_q^k|3m'\rangle$, where $C_q^k = [4\pi/(2k+1)]^{1/2}Y_{kq}$, and are the standard Racah tensor operators expressed in terms of the spherical harmonics. These matrix elements were then expressed as

$$\langle 3m|C_q^k|3m'\rangle = (-1)^{3-m}\begin{pmatrix} 3 & k & 3 \\ -m & q & m' \end{pmatrix}\langle 3\|C^k\|3\rangle, \quad (13)$$

and the $3j$ symbols are nonzero unless $3+k+3$ is even ($k=6,4,2,0$) and $q=m-m'$. The leading central metal ion multipoles are for $k=6$, 4, and 2, but the $k=6$ contribution is negligible.

C. Total oscillator strength of the vibronic transition

We have confined the calculations to the leading multipoles $k=1$ and $k=3$ for the CF term, and to $k=2$ and $k=4$ for the LP term. The resulting electronic factors are tabulated in Appendix B. As expected, the $k=3$ and $k=4$ contribution terms to the vibronic intensity are found to be 1–2 orders of magnitude smaller than the leading contribution terms, and this may be regarded as a reasonable justification for the neglect of higher-order terms. The leading (dipolar) contribution of the CF term to the vibronic intensity of the $\nu_6(\tau_{2u})$ vibronic origins is, however, zero.

The calculated oscillator strength, P_{if}, for the vibronic transition $f \leftarrow i$ is given by the equation

$$P_{if} = \frac{8\pi^2 mc}{3hg_0e^2}\chi\overline{\nu}\sum_f |\langle i|\mu^\alpha|f\rangle|^2 = 1.0847\times10^{15}\chi\overline{\nu}D_{if}e^{-2}g_0^{-1}, \quad (14)$$

where D_{if} is the dipole strength in C^2m^2; e is the electron charge, in C; g_o is the degeneracy of the initial state (i.e., two for Γ_6); $\overline{\nu}$ is the ZPL wave number of the electronic transition; and χ is the effective field correction[46] for an absorptive transition, approximated by $\chi=(n^2+2)^2/9n$. Considering the $({}^2F_{5/2})\Gamma_8,\Gamma_7 \leftarrow \Gamma_6({}^2F_{7/2})$ excitations for which the ZPL wave numbers are 10 246±2 cm^{-1} (to Γ_8) and 10 717±2 cm^{-1} (to Γ_7) at 20 K, the use of Eq. (3) gives values of χ of 1.439 and 1.441, respectively.

Factoring (14) into electronic and vibrational integrals, we can write the oscillator strengths for individual vibronic origins:

$$P(\nu_3) = 1.0847\times10^{15}\chi\overline{\nu e}^{-2}g_0^{-1}|\langle 0|Q_3|1\rangle|^2(U_3L_{33}+U_4L_{43})^2, \quad (15a)$$

$$P(\nu_4) = 1.0847\times10^{15}\chi\overline{\nu e}^{-2}g_0^{-1}|\langle 0|Q_4|1\rangle|^2(U_3L_{34}+U_4L_{44})^2, \quad (15b)$$

$$P(\nu_6) = 1.0847\times10^{15}\chi\overline{\nu e}^{-2}g_0^{-1}|\langle 0|Q_6|1\rangle|^2(U_6L_{66})^2, \quad (15c)$$

where the vibrational integrals involving a difference of one quantum are calculated (in m^2) under the harmonic approximation:

$$|\langle 0|Q_i|1\rangle|^2 = (h/8\pi^2c\overline{\nu_i})^{1/2}/1.672\,623\,1\times10^{-27}, \quad (16)$$

and the electronic factors are calculated from the tabulation in Appendix B by

$$U_i^\alpha = U_i^\alpha(\mathrm{CF}) + U_i^\alpha(\mathrm{LP}). \quad (17)$$

D. Vibrational equation of motion

The next step in the vibronic intensity calculation is to replace the set of symmetry coordinates, S_{kt}, by the normal coordinates of the system, Q_{kt}, by using the transformation $S=LQ$.[47] The correct choice of phase is essential, and this has been discussed by Acevedo, Vásquez, and Passman.[48] We follow the standard procedure by solving $GFL=L\Lambda$, where $G=LL'$, so that $\Lambda=L'FL$. It then follows that the diagonal elements of the matrix Λ are given by

$$\lambda_i = \sum_k L_{ki}^2F_{kk} + \sum_{k,l} L_{kl}L_{li}F_{kl}. \quad (18)$$

We have calculated the potential-energy distribution (PED) by two different approaches. First, following the customary approach in neglecting the off-diagonal elements F_{kl} with respect to the diagonal matrix elements F_{kk} (this calculation method is labeled NEG hereafter). Second, we have modeled the short-range interactions using as an additional criterion the minimization of the crossterm, $(\mathrm{CT})_{\nu_i}$:

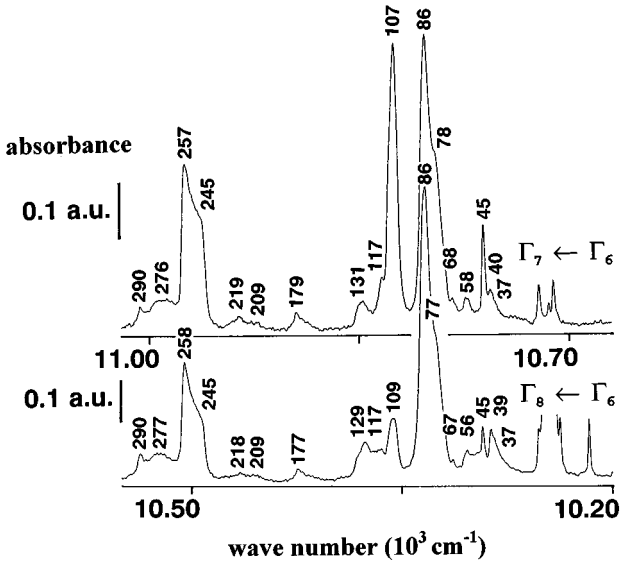

FIG. 1. 20-K absorption spectrum of $Cs_2NaYbCl_6$ between 10 200 and 11 000 cm^{-1}. The wave number displacements of vibronic structure from the $\Gamma_7 \leftarrow \Gamma_6$ electronic origin (inferred to be at 10 717±2 cm^{-1}) and from the $\Gamma_8 \leftarrow \Gamma_6$ origin (10 246±2 cm^{-1}) are indicated. The region near the $\Gamma_8 \leftarrow \Gamma_6$ electronic origin has been truncated for clarity.

$$(\mathrm{CT})_{\nu_i} = \sum_{k,l} L_{ki} L_{li} F_{kl} \quad \text{for } k \text{ other than } i, \qquad (19)$$

this calculation method being labeled MIN hereafter. These different methods were used, together with the employment of different vibrational force fields, in order to investigate the consequent changes in the L matrices. In calculation NEG, the wave numbers of the ν_3 and ν_4 modes were calculated from the vibronic sidebands by averaging over the longitudinal optic (LO) and transverse optic (TO) mode wave numbers:

$$3\overline{\nu_i^2} = [\overline{\nu_i}(\mathrm{LO}) + 2\overline{\nu_i}(\mathrm{TO})]^2 \quad \text{for } i = 3 \text{ and } 4, \qquad (20)$$

whereas in the MIN calculation the TO mode wave numbers were employed in the normal coordinate calculations.

IV. APPLICATION TO $YbCl_6^{3-}$

Malta has described the interaction between a rare-earth ion CF level and a vibronic level,[11] and noted that two bands of comparable intensity may appear in the optical spectra in such a case when the vibronic coupling is strong and the levels are resonant. Resonance between an electronic level and a vibronic level has been identified in the electronic spectra of Pr^{3+} doped into elpasolite lattices.[49] In the case of $Cs_2NaYbCl_6$, resonance occurs between the $(^2F_{5/2})\Gamma_8$ CF level and the $(^2F_{5/2})\Gamma_6 + \nu_2$ vibronic level, where the vibration is of *even* parity, and we are at present studying this. This work has therefore concentrated upon the absorption spectrum of $Cs_2NaYbCl_6$, where such complications are absent.

Figure 1 shows the 20-K absorption spectrum of $Cs_2NaYbCl_6$, with the higher-energy $(^2F_{7/2})\Gamma_7 \leftarrow \Gamma_6(^2F_{5/2})$ group of bands superimposed upon the lower-energy $(^2F_{7/2})\Gamma_8 \leftarrow \Gamma_6(^2F_{5/2})$ group. The wave-number displacements of the vibronic origins from the observed or inferred positions of the ZPL are marked. In the present study we are only concerned with the $S_6(\nu_3)$, $S_7(\nu_4)$, and $S_{10}(\nu_6)$ vibronic origins, and the assignment of these to structure with maxima near 257, 108, and 86 cm^{-1}, respectively, is taken from Ref. 50. Barbanel *et al.* have associated the multiple structure of vibronic origins with multiple electronic transitions, occurring due to nonequivalence of crystallographic positions at low temperature.[51] We do not concur with this because the derived vibrational wave numbers in Fig. 1 are the same for both transitions, but the ''ZPL splittings'' [51] are not the same, and furthermore the multiple structure attributed to vibronic origins is observed for other lanthanide elpasolites at similar wave numbers.

TABLE I. Calculated L matrix elements for $YbCl_6^{3-}$ in $Cs_2NaYbCl_6$.

Type of force field	L_{33}	L_{34}	L_{43}	L_{44}
GVFF5,[a] NEG	0.1992	0.0091	−0.1294	0.2931
GVFF5,[a] MIN	0.199	0.01	−0.132	0.292
GVFF29,[b] NEG	0.1945	0.0440	−0.1790	0.2657
MUBFF,[c] NEG	0.198	−0.0219	−0.0823	0.3096
MOVFF,[d] NEG	0.1962	−0.0354	−0.0610	0.3145

[a]Five-parameter general valence force field, with same assumptions as Ref. 52.
[b]29-parameter fit including all GVFF interaction force constants (Ref. 53).
[c]Modified Urey-Bradley force field.
[d]Modified orbital valence force field.
NEG neglecting off-diagonal elements F_{kl} with respect to F_{kk}; MIN minimizing cross term, Eq. (19).

The calculated τ_{1u} mode L matrix elements for $YbCl_6^{3-}$ in $Cs_2NaYbCl_6$ are listed in Table I, the magnitude of L_{66} being simply $G_6^{1/2}$. The two approaches used in the five-parameter general valence force field (GVFF) (Ref. 52) give very similar matrix elements. The more complete force-field GVFF29,[53] which includes all angle-angle, bend-bend, and angle-bend interaction constants gives off-diagonal matrix elements with larger magnitude, whereas some changes of sign also occur in the modified Urey-Bradley force field (MUBFF) and the modified orbital valence force field (MOVFF).

The measured oscillator strengths of vibronic origins in the $(^2F_{7/2})\Gamma_8, \Gamma_7 \leftarrow \Gamma_6(^2F_{5/2})$ transitions of $YbCl_6^{3-}$ are collected in Table II. The values are in the range 10^{-8}–10^{-9}, with a precision of about 10%. Each vibronic origin consists of multiple structure, and there are alternative assignments to zone boundary (ZB) structure and LO modes in several cases. For example, the ν_4 LO mode is essentially coincident with the ν_5 ZB mode. Two alternative band integration schemes are labeled A and B in the table. The measured oscillator strengths in A and B are reasonably similar, with all vibronic origins making a comparable contribution to the intensity, and $(^2F_{7/2})\Gamma_8 + \nu_4 \leftarrow \Gamma_6(^2F_{5/2})$ being weakest.

A. Calculations including relaxation of the closure approximation

The calculated oscillator strengths of vibronic origins in the $(^2F_{7/2})\Gamma_8, \Gamma_7 \leftarrow \Gamma_6(^2F_{5/2})$ transitions are also listed in

TABLE II. Calculated and measured vibronic oscillator strengths for $YbCl_6^{3-}$.

	$\Gamma_8 \leftarrow \Gamma_6$			$\Gamma_7 \leftarrow \Gamma_6$		
	ν_3	ν_4	ν_6	ν_3	ν_4	ν_6
Measured oscillator strengths $\times 10^9$ [a]						
Measured ratios						
A	18.3(2.0)[b]	5.4(0.8)	40.2(4.6)	20.7(2.1)	18.6(2.0)	32.0(3.4)
	0.46	0.14	1.00	0.52	0.46	0.80
B	27.6(3.2)	12.8(1.2)	40.2(4.6)	26.8(2.3)	23.3(2.5)	32.0(3.4)
	0.69	0.32	1.00	0.67	0.58	0.80
C	20.6	<3.7	31.0	23.2	22.1	27.8
	0.67	<0.12	1.00	0.75	0.71	0.90
Calculated oscillator strengths $\times 10^9$ [a]						
Calculated ratios						
Relaxation of the closure approximation:						
GVFF5, NEG	1.58	1.54	2.72	2.99	0.36	3.57
	0.58	0.56	1.00	1.10	0.13	1.31
GVFF5, MIN	1.58	1.54	2.72	3.00	0.35	3.57
	0.58	0.56	1.00	1.10	0.13	1.31
GVFF29, NEG	1.55	1.61	2.72	3.15	0.02	3.57
	0.57	0.59	1.00	1.15	0.007	1.31
MUBFF, NEG	1.56	1.39	2.72	3.15	0.99	3.57
	0.57	0.51	1.00	1.15	0.36	1.31
MOVFF, NEG	1.54	1.31	2.72	2.71	1.35	3.57
	0.56	0.48	1.00	0.99	0.49	1.31
Invoking the closure approximation:[c]						
MUBFF, NEG	0.84	0.80	2.99	13.6	2.70	2.63
	0.28	0.27	1.00	4.55	0.90	0.88

[a]Oscillator strengths are given on the first line for each measurement or force field, and the ratios with respect to $\Gamma_8+\nu_6 \leftarrow \Gamma_6$ are given underneath in small type.

[b]The ± measured values are given in parentheses from crystals of three different thicknesses, at 20 K. *A*, *B* from $Cs_2NaYbCl_6$; *B* includes LO and ZB contributions of bands near 117, 131 cm^{-1} to ν_4, and near 276, 290 cm^{-1} to ν_3 in addition to the bands at 108 cm^{-1} (ν_4) and 245, 257 cm^{-1} (ν_3) measured in *A*. Bands at 78, 86 cm^{-1} were integrated for the oscillator strength of ν_6 in both cases. *C* measured from the 20-K absorption spectrum of $Cs_2NaGd_{0.97}Yb_{0.03}Cl_6$.

[c]With parameters $c_1=c_2=1.0/6.0$.

Table II. The values are smaller than from experiment but agree within an order of magnitude. The L_{66} matrix element in (15c) is independent of the force field and the intensity ratio of the ν_6 vibronic origins in the absorption transitions to the Γ_7 and Γ_8 upper levels is calculated to be 1.31:1, respectively, whereas the measured ratio is 0.80:1. This agreement is satisfactory in the framework of the model since no variable parameters have been introduced.

The calculated intensity ratios of the vibronic origins [with respect to $(^2F_{7/2})\Gamma_8+\nu_6 \leftarrow \Gamma_6(^2F_{5/2})$] are generally similar when using the different force fields, with the exception of $(^2F_{7/2})\Gamma_7+\nu_4 \leftarrow \Gamma_6(^2F_{5/2})$. In this case the agreement is better using MUBFF and MOVFF rather than GVFF. It is interesting that the GVFF29 force field, which produces the best agreement with experimental vibrational wave numbers, produces the poorest fit to the vibronic intensities due to the cancellation of U_3L_{34} and U_4L_{44} terms in (15b).

B. Calculations invoking the closure approximation

Judd[54] and Ofelt[55] have utilized a simplification in evaluating matrix elements which collapses two odd-parity operators D^1_p and D^1_q into the even-rank tensor operator U^2_{p+q}, with certain assumptions. When the Judd-Ofelt closure approximation is utilized, the expression for the θth vector component of the transition dipole moment is

$$\mu^{\mathrm{CF},\theta}({}^2F_{5/2}\Gamma_x\gamma_x\leftarrow\Gamma_6\gamma_6{}^2F_{7/2})=\frac{2Ze}{\Delta E}\sum_{kt}S_{kt}\sum_{\Gamma\gamma}\sum_{i\tau}A_{kt}^{\Gamma\gamma}(i,\tau)\langle{}^2F_{7/2}\Gamma_6\gamma_6|M_{\gamma}^{\Gamma}(i,\tau)\mu^{\theta}|{}^2F_{5/2}\Gamma_x\gamma_x\rangle, \tag{21}$$

based upon the complete utilization of closure over the central metal ion intermediate states, i.e.,

$$\sum_{i=1}^{\infty}|i\rangle\langle i|=1. \tag{22}$$

In this study we have used a truncated expansion over the intermediate states, so that for the restricted basis set (22) should be rewritten as

$$\sum_{i=1}^{N}|i\rangle\langle i|=c, \tag{23}$$

where c is a positive number less than unity. The right-hand side of (22) is therefore modified by multiplication by this coefficient, as is the associated electronic factor, $U_{kt}^{\mathrm{CF},\theta}(clo)$:

$$U_{kt}^{\mathrm{CF},\theta}(clo)=c\,\frac{2Ze}{\Delta E}\sum_{\Gamma\gamma}\sum_{i\tau}A_{kt}^{\Gamma\gamma}(i,\tau)\langle{}^2F_{7/2}\Gamma_6\gamma_6|M_{\gamma}^{\Gamma}(i,\tau)\mu^{\theta}|{}^2F_{5/2}\Gamma_x\gamma_x\rangle. \tag{24}$$

Furthermore, the tensorial product may be written as

$$\mu^{\theta}M_{\gamma}^{\Gamma}(i,\tau)=\sum_{\Gamma\overline{\gamma}}\lambda(\overline{\Gamma})^{1/2}(-1)^{\overline{\Gamma}+\overline{\gamma}^{+}}V\begin{pmatrix}T_1 & \Gamma & \overline{\Gamma}\\ \theta & \gamma & \overline{\gamma^{+}}\end{pmatrix}O_{\overline{\gamma}}^{\overline{\Gamma}}(T_1\Gamma|i,\tau), \tag{25}$$

where the symmetry-adapted coefficients are given by

$$O_{\overline{\gamma}}^{\overline{\Gamma}}(T_1\Gamma|i,\tau)=\sum_{k,q}P^{\overline{\Gamma}\,\overline{\gamma}}(T_1\Gamma|i,\tau)C_q^k. \tag{26}$$

Both the crystal-field electronic factors and the total electronic factors associated with the zth vector component of the transition dipole moments are listed in Appendix B. The coefficients c_1 (occurring in the electronic factors for transitions to the Γ_7 excited state) and c_2 (for transitions to Γ_8) are a consequence of using the truncated basis set (23), and could be formally evaluated by taking all intermediate states into account, but this would be a formidable task. The closure approximation calculation results, utilizing the MUBFF and values of c_1 and c_2 equal to 1/6, are presented in Table II. The current choice is intended to be illustrative, not definitive, and was made from the comparison of both the CF (without invoking closure) and the LP electronic factors. All values of vibronic oscillator strengths, with the notable exception of $\Gamma_7+\nu_3\leftarrow\Gamma_6$, are within a factor of 2 of the results from closure relaxation. It is more instructive to investigate the sensitivity of the calculated vibronic oscillator strengths to the parameters c_i $(i=1,2)$, choosing conditions when the nature of the force field has no effect upon the result. The ratio (R) of the oscillator strengths of ν_6 vibronic origins in the $\Gamma_8\leftarrow\Gamma_6$ and $\Gamma_7\leftarrow\Gamma_6$ transitions is plotted against the magnitudes of the c_i parameters in Fig. 2. The resulting simple three-dimensional (3D) surface shows that the transition $\Gamma_8+\nu_6\leftarrow\Gamma_6$ is stronger than $\Gamma_7+\nu_6\leftarrow\Gamma_6$ (by up to 19.4 times when $c_1=c_2=1$), and that the ratio is more sensitive to the value of c_1 rather than c_2.

C. Vibronic oscillator strengths of dilute $Cs_2NaGdCl_6$: $YbCl_6^{3-}$

We have investigated the vibronic oscillator strengths of $YbCl_6^{3-}$ diluted into a transparent host lattice for two reasons. First, there is current interest in the concentration dependence of vibronic intensities: some authors claiming enhancement of vibronic intensity with concentration as a result of ion-pair interactions[56,57] or enhanced electron-phonon interaction in the excited state[58] whilst others dispute this.[59,60] In Fig. 3 the total vibronic intensities of the $({}^2F_{7/2})\Gamma_8\leftarrow\Gamma_6({}^2F_{5/2})$ and $({}^2F_{7/2})\Gamma_7\leftarrow\Gamma_6({}^2F_{5/2})$ transitions are plotted against the mole fraction of Yb^{3+} (with respect to Gd^{3+}) in $Cs_2NaYb_xGd_{1-x}Cl_6$, taking into account the variation in lattice parameter and the crystal thickness. The oscillator strengths are (as defined) independent of Yb^{3+} concentration, so that the model of an isolated $YbCl_6^{3-}$ moeity is valid.

The second reason for the investigation of the mixed crystals was for the comparison of the intensities of the individual vibronic origins with calculated data. Phonon dispersion is generally smaller in diluted crystals so that the vibronic selection rules approximate more closely to $\mathbf{k}=0$. The vibronic spectra of $Cs_2NaYb_xGd_{1-x}Cl_6$ $(x=0.9$–$0.1)$ exhibit band splittings in the $\Gamma_8\leftarrow\Gamma_6$ transition, but not in the $\Gamma_7\leftarrow\Gamma_6$ transition, attributed to site symmetry splitting of the Γ_8 state into two Kramers doublets. At low Yb^{3+} concentrations $(x<0.1)$ the ZPL and vibronic splittings are not resolved. Individual vibronic intensities are listed in Table II (C) for the most dilute crystal studied, for comparison with calculation, and the values are generally similar to those from the neat crystals in A and B. The Yb-diluted $Cs_2NaGdCl_6$ crystals exhibit similar multiple structure for each vibronic vibronic origin as in *neat* $Cs_2NaYbCl_6$, the

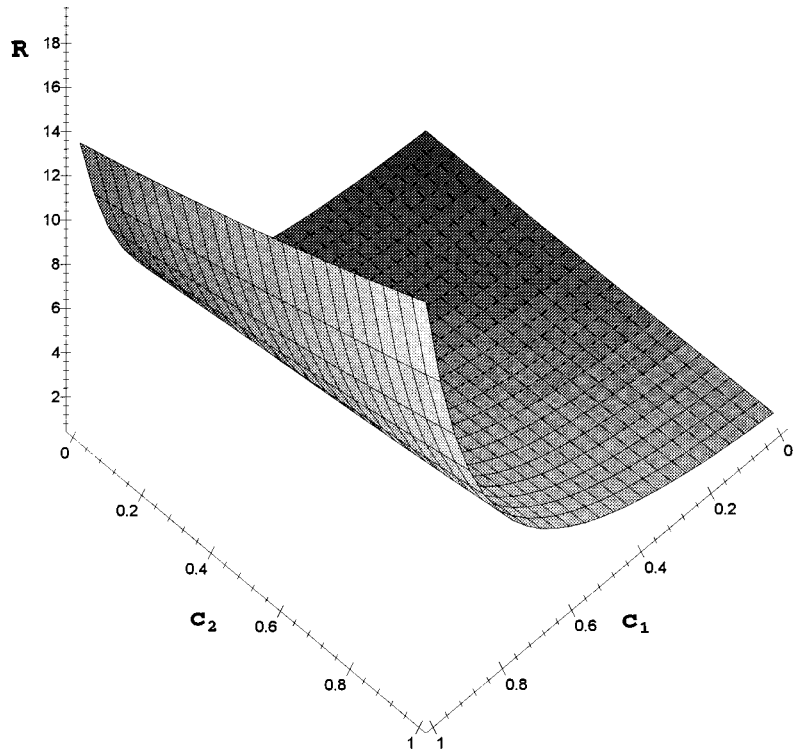

FIG. 2. Plot of the ratio, R, of the oscillator strengths $P(\Gamma_8+\nu_6\leftarrow\Gamma_6)/P(\Gamma_7+\nu_6\leftarrow\Gamma_6)$ against the closure approximation parameters c_1 and c_2.

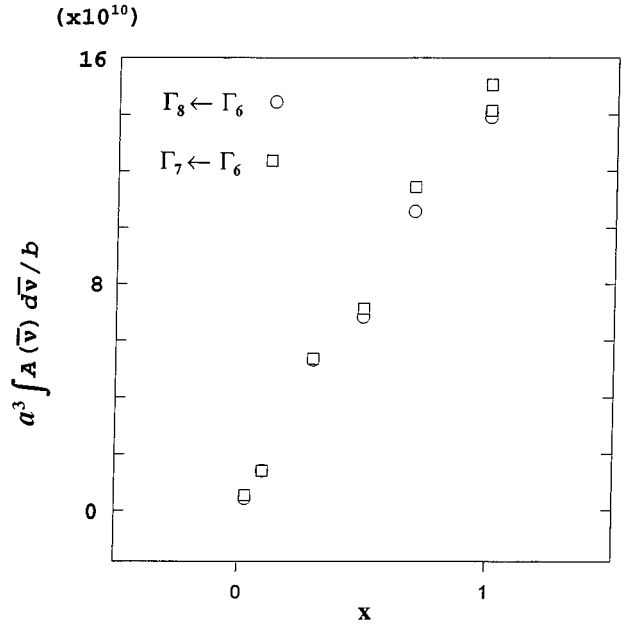

FIG. 3. Total vibronic intensities of the $\Gamma_8,\Gamma_7\leftarrow\Gamma_6$ transitions in the 20-K absorption spectra of $Cs_2NaGd_{1-x}Yb_xCl_6$ as a function of x, the mole fraction of Yb in the crystal. The slope of the plot of $\alpha^3\int A(\overline{\nu})d\overline{\nu}/b$ $(=y)$ against x [where α, the interpolated unit cell parameter, is in pm, b in cm, and $\int A(\overline{\nu})d\overline{\nu}$ in cm^{-1}] is given by 1.5377×10^{18} P, where P is the total vibronic oscillator strength of the transition. The coefficients of linear regression are the $R=0.996$ and 0.998 for the plots of the $\Gamma_7\leftarrow\Gamma_6$ and $\Gamma_8\leftarrow\Gamma_6$ transitions, and the derived values of $P/10^{-8}$ are 9.6 and 9.2, respectively.

moeity-mode wave numbers differing by very little for the $Cs_2NaYbCl_6$ and $Cs_2NaGdCl_6$ host crystals.

V. COMPARISON WITH OTHER Yb^{3+} SYSTEMS

For comparison with the spectral data from $Cs_2NaYbCl_6$, two other systems were investigated, although for reasons given later, quantitative vibronic intensity calculations have not been performed. Figure 4 shows the Raman spectra of $Cs_2LiYbCl_6$ and Cs_2KYbF_6 and there is no evidence of distortion from octahedral symmetry of the YbX_6^{3-} moeity (X =Cl,F) in either case. In Fig. 5 the vibronic sidebands in the electronic absorption spectra of these two compounds are shown. The vibronic structure is broader and more complex in the spectrum of $Cs_2LiYbCl_6$ than that of $Cs_2NaYbCl_6$, and this is attributed to two reasons. First, the dispersion of vibrational modes is more pronounced: for example, the ZB ν_1 and ν_5 modes appear more prominently in the absorption spectra, with wave numbers similar to the Raman-active zone-center (ZC) modes (Figs. 4 and 5). Second, the intensity of the τ_{1u} lattice mode associated with lithium motion is much stronger in the sidebands of $Cs_2LiYbCl_6$, compared with the sodium mode in $Cs_2NaYbCl_6$. The wave number of the ''lithium mode'' is much higher so that mixing of the external mode symmetry coordinate with the Yb-Cl antisymmetric stretch coordinate is much greater than in $Cs_2NaYbCl_6$. These considerations apart, it is evident that all six internal mode vibronic origins contribute substantial intensity to the sidebands, with $\Gamma_8+\nu_4\leftarrow\Gamma_6$ being weakest. Figure 5(b) depicts the $(^2F_{7/2})\Gamma_7\leftarrow\Gamma_6(^2F_{5/2})$ sideband of Cs_2KYbF_6. The electronic origin, which is electric quadrupole allowed under O_h molecular point group selection rules, appears relatively strong. This probably indicates an electric-dipole contribution to the ZPL intensity from the presence of a larger number of defect sites in the crystal. Becker *et al.*[30]

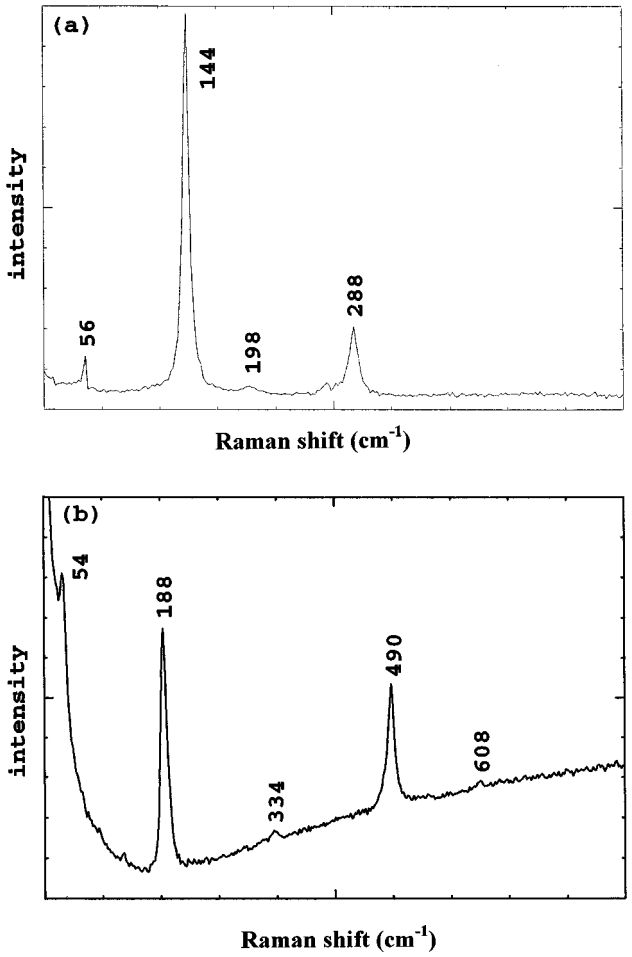

FIG. 4. 514.5-nm excited Raman spectra of YbX_6^{3-}: (a) 120-K spectrum of $Cs_2LiYbCl_6$; and (b) 20-K spectrum of Cs_2KYbF_6.

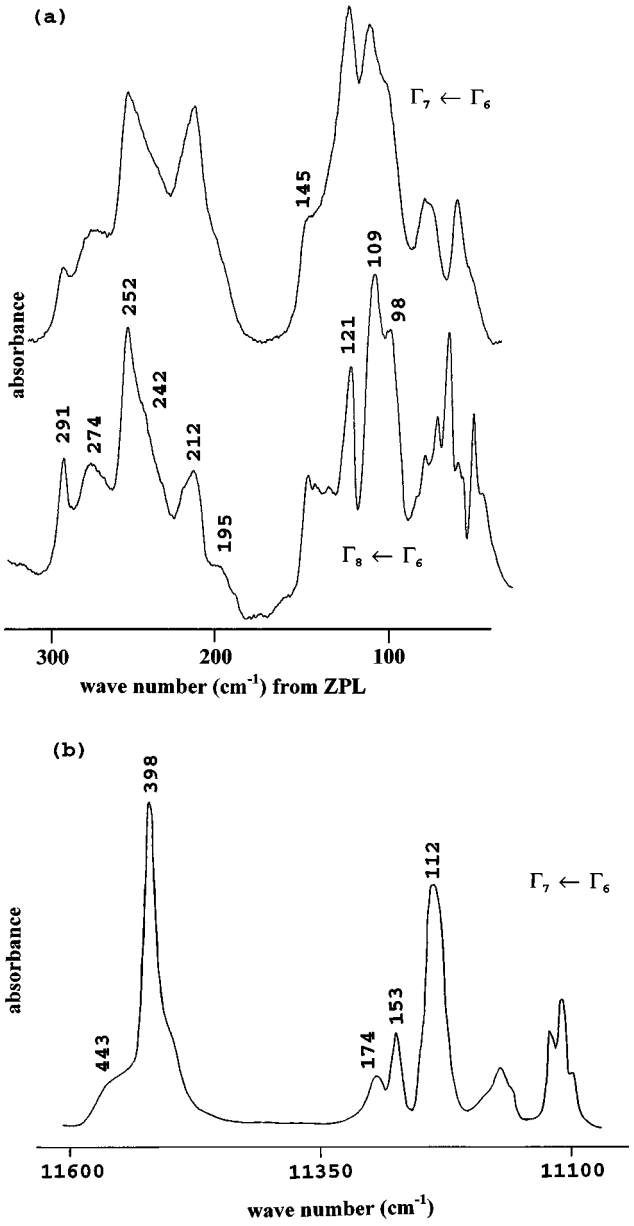

FIG. 5. 20-K vibronic spectra of YbX_6^{3-}: (a) The Γ_8, $\Gamma_7 \leftarrow \Gamma_6$ sidebands of $Cs_2LiYbCl_6$; (b) the $\Gamma_7 \leftarrow \Gamma_6$ sideband of Cs_2KYbF_6. The $(^2F_{7/2})\Gamma_8, \Gamma_7 \leftarrow \Gamma_6(^2F_{5/2})$ electronic origins are at 10 238 and 10 705 cm^{-1} in (a), and at 10 400 and 11 120 cm^{-1} in (b). The wave-number displacements of the vibronic structure from the zero-phonon line are indicated in (a).

have reported the room-temperature infrared spectrum of Cs_2KYbF_6, and the infrared window between 70 and 150 cm^{-1} enables the assignment of the τ_{2u} mode at 115 ± 3 cm^{-1} from the vibronic sideband. Three *infrared* bands observed at 156, 176, and 392 cm^{-1}, corresponding to $\mathbf{k}=0$ τ_{1u} modes, have counterparts in the vibronic sideband. The two features at 153 and 174 cm^{-1} in Fig. 5(b) thus correspond to strongly mixed internal (S_7,ν_4) and external (S_8) modes. The lowest-energy vibronic structure near 50 and 72 cm^{-1} above the inferred position of the electronic origin, are ZB lattice modes correlating with the $\mathbf{k}=0$ τ_{2g} and τ_{1u} modes observed at 54 and 70 cm^{-1} in the Raman and infrared spectra, respectively.

The spectral manifestations of the extensive mixing of internal and external vibrational modes in $Cs_2LiYbCl_6$ and Cs_2KYbF_6 indicate that consideration of the entire unit cell be taken into account in the vibronic intensity calculations, so that we have not applied the present model to these cases.

VI. CONCLUSIONS

The oscillator strengths and intensity ratios of individual vibronic origins in the absorption spectrum of $Cs_2NaYbCl_6$ have been reproduced to within an order of magnitude by vibronic intensity calculations utilizing a model of the isolated chromophore $YbCl_6^{3-}$. Calculated vibronic oscillator strengths exhibit sensitivity to the vibrational force field employed, arising from cancellations in sums of U_iL_{kl} terms; and to the method of calculation of the electronic factors, U_i. The *measured* oscillator strengths for neat $Cs_2NaYbCl_6$ are somewhat greater than the calculated values, which could indicate the importance of contributions to the vibronic intensity from points away from the zone center. However, the *measured* oscillator strengths are similar for both $Cs_2NaYbCl_6$ and $Cs_2NaGdCl_6$: $YbCl_6^{3-}$. Examples of vibronic sidebands have also been presented to show the redistribution of moeity mode vibronic intensity to lattice mode bands, *via* the mixing of vibrational symmetry coordinates. Calculations are in progress which will take the above factors into account.

ACKNOWLEDGMENTS

We thank Jason Krishnan for technical assistance, and Dr. Liu Yu-long for recording the Raman spectra. P.A.T. acknowledges support under HKUPGC RG#904098; R.A. would like to thank both Fondecyt, Grant No. 1950668, and the Chilean Nuclear Energy Commission for financial support.

APPENDIX A

Note: The O double group representation labels Γ_6, Γ_7, Γ_8 are used interchangeably with E', E'', U' respectively, in this work.

1. Reduced matrix elements in the crystal-field calculation: Relaxation of the closure approximation

$\langle {}^2F_{7/2}(f^{13})||C^1||L'\ \frac{1}{2}\ J(f^{12}d)\rangle\langle L'\ \frac{1}{2}\ J(f^{12}d)||C^k||{}^2F_{5/2}(f^{13})\rangle$

$^2G_{9/2}$		$^2G_{7/2}$		$^2F_{7/2}$		$^2F_{5/2}$		$^2D_{5/2}$	
$k=1$	$k=3$	$k=1$	$k=3$	$k=1$	$k=3$	$k=1$	$k=3$	$k=1$	$k=3$
$-$	$\frac{10\sqrt{154}}{147}$	$\frac{66\sqrt{3}}{49}$	$\frac{44}{147}$	$\frac{-90\sqrt{3}}{49}$	$\frac{108}{147}$	$\frac{-60\sqrt{5}}{49}$	$\frac{2\sqrt{30}}{49}$	$\frac{276\sqrt{5}}{245}$	$\frac{24\sqrt{30}}{245}$

$\langle {}^2F_{7/2}(f^{13})||C^3||L'\ \frac{1}{2}\ J'(f^{12}d)\rangle\langle L'\ \frac{1}{2}\ J'(f^{12}d)||C^1||{}^2F_{5/2}(f^{13})\rangle$

$^2G_{7/2}$	$^2F_{7/2}$	$^2F_{5/2}$	$^2D_{5/2}$	$^2D_{3/2}$
$\frac{12\sqrt{11}}{49}$	$\frac{4\sqrt{11}}{49}$	$\frac{8\sqrt{15}}{49}$	$\frac{12\sqrt{15}}{245}$	$\frac{12\sqrt{7}}{245}$

2. The $Z_k^{\Gamma}(\Gamma_1 J_1|\Gamma_2 J_2)$ coefficients: Crystal-field calculation, relaxation of the closure approximation

$\Gamma=T_1$, $k=1$

	$E'_{7/2}$	$E''_{7/2}$	$U'_{7/2}$	$E''_{5/2}$	$U'_{5/2}$
$E'_{7/2}$	$\sqrt{21}/18$	0	$\sqrt{15}/9$	0	$-1/2$
$E''_{7/2}$	0	$-\sqrt{21}/14$	$-\sqrt{7}/7$	$-2\sqrt{21}/21$	$-\sqrt{105}/42$
$U'_{7/2}$	$-\sqrt{15}/9$	$-\sqrt{7}/7$	$(1)-\sqrt{210}/630$	$-\sqrt{7}/7$	$(1)-\sqrt{14}/7$
	0	0	$(2)-\sqrt{210}/35$	0	$(2)-\sqrt{14}/14$
$E''_{5/2}$	0	$2\sqrt{21}/21$	$\sqrt{7}/7$	$\sqrt{35}/21$	$-4\sqrt{7}/21$
$U'_{5/2}$	1/2	$-\sqrt{105}/42$	$(1)\sqrt{14}/7$	$-4\sqrt{7}/21$	$(1)-\sqrt{14}/14$
	0	0	$(2)\sqrt{14}/14$	0	$(2)\sqrt{14}/14$

and also

	$E'_{9/2}$	$U'^{a}_{9/2}$	$U'^{b}_{9/2}$
$E'_{7/2}$	$2\sqrt{3}/9$	$\sqrt{6}/12$	$\sqrt{14}/12$
	$E''_{5/2}$	$U'_{5/2}$	$U'_{5/2}$
$U'_{3/2}$	$-\sqrt{3}/3$	(1)0	$(2)-\sqrt{6}/3$

$\Gamma=T_1$, $k=3$

	$E'_{7/2}$	$E''_{7/2}$	$U'_{7/2}$	$E''_{5/2}$	$U'_{5/2}$	$U'_{3/2}$
$E'_{9/2}$	0	0	0	0	$-\sqrt{66}/66$	0
$U'^{a}_{9/2}$	0	0	0	$-\sqrt{165}/66$	$(1)4\sqrt{330}/165$	0
$U'^{a}_{9/2}$	0	0	0	0	$(2)-\sqrt{330}/330$	0
$U'^{b}_{9/2}$	0	0	0	$-3\sqrt{385}/154$	$(1)-2\sqrt{770}/385$	0

$U'^{b}_{9/2}$	0	0	0	0	$(2)\sqrt{770}/770$	0
$E'_{7/2}$	$\sqrt{77}/33$	0	$\sqrt{55}/66$	0	$\sqrt{3}/6$	$-\sqrt{6}/12$
$E''_{7/2}$	0	$\sqrt{77}/22$	$-3\sqrt{231}/154$	$-\sqrt{7}/14$	$\sqrt{35}/14$	0
$U'_{7/2}$	0	0	0	$-\sqrt{21}/42$	$(1)-\sqrt{42}/21$	0
$U'_{7/2}$	0	0	0	0	$(2)-\sqrt{42}/42$	0
$E''_{5/2}$	0	0	0	$-2\sqrt{210}/63$	$-\sqrt{42}/126$	0
$U'_{5/2}$	0	0	0	$-\sqrt{42}/126$	$(1)-2\sqrt{21}/21$	0
$U'_{5/2}$	0	0	0	0	$(2)-2\sqrt{21}/63$	0

$\Gamma=T_2$, $k=3$

	$E'_{7/2}$	$E''_{5/2}$	$U'_{7/2}$	$U'_{5/2}$	$U'_{3/2}$
$E'_{9/2}$	0	$-4\sqrt{66}/99$	0	$13\sqrt{330}/990$	0
$E'_{7/2}$	0	$\sqrt{3}/18$	$-\sqrt{11}/22$	$\sqrt{15}/18$	$-\sqrt{30}/24$
$U'^{a}_{9/2}$	0	$-5\sqrt{33}/198$	0	$(1)-13\sqrt{330}/1320$	0
$U'^{a}_{9/2}$	0	0	0	$(2)-\sqrt{330}/88$	0
$U'^{b}_{9/2}$	0	$\sqrt{77}/44$	0	$(1)\sqrt{770}/88$	0
$U'^{b}_{9/2}$	0	0	0	$(2)17\sqrt{770}/1540$	0
$U'_{7/2}$	0	$-5\sqrt{105}/126$	0	$(1)2\sqrt{42}/63$	0
$U'_{7/2}$	0	0	0	$(2)-\sqrt{42}/18$	0
$U'_{5/2}$	0	$-\sqrt{210}/42$	0	$(1)-2\sqrt{21}/2$	0
$U'_{5/2}$	0	0	0	(2)0	0

APPENDIX B

Crystal-field and ligand polarization electronic factors for the $\mu^z[^2F_{5/2}\Gamma_7,\Gamma_8\leftarrow\Gamma_6{}^2F_{7/2}]$ electronic transitions of $Cs_2NaYbCl_6$ (in units of 10^{-4} electron charge).

The radial integrals chosen were as follows:[54] $\langle r\rangle_{fd}=0.292\times10^{-10}$ m; $\langle r^3\rangle_{fd}=0.318\times10^{-30}$ m^3; $\langle r^2\rangle_{ff}=0.1933\times10^{-20}$ m^2; $\langle r^4\rangle_{ff}=0.0932\times10^{-40}$ m^4.

1. Without invoking closure

Crystal-field electronic factors, $U^{\mathrm{CF},Z}$:

	$E''\beta''$	U'_κ	U'_λ	U'_μ	U'_ν
ν_3	−3.627	−8.339	−3.533	−5.690	0
ν_4	−2.987	−2.219	−1.453	−3.198	0
ν_6	0.387	−2.957	0	−0.770	0.451

Ligand polarization electronic factors, $U^{\mathrm{LP},Z}$:

	$E''\beta''$	U'_κ	U'_λ	U'_μ	U'_ν
ν_3	−29.653	−6.655	11.279	−17.532	0
ν_4	9.991	5.324	−7.204	−4.876	0
ν_6	19.662	5.573	0	−13.997	−10.262

Total electronic factors, $U^{(\mathrm{CF+LP}),Z}$:

	$E''\beta''$	U'_κ	U'_λ	U'_μ	U'_ν
ν_3	−33.280	−14.994	7.746	−23.222	0
ν_4	7.004	3.105	−8.657	−8.074	0
ν_6	20.049	2.616	0	−14.767	−9.811

2. With the closure approximation

Crystal-field electronic factors $U_{kt}^{\mathrm{CF},\theta}(clo)$:

	$E''\beta''$	U'_κ	U'_λ	U'_μ	U'_ν
ν_3	$34.640c_1$	$19.280c_2$	$10.447c_2$	$26.114c_2$	0
ν_4	$22.775c_1$	$6.760c_2$	$6.336c_2$	$14.437c_2$	0
ν_6	$-14.812c_1$	$-2.940c_2$	0	$-3.733c_2$	$-2.262c_2$

Total electronic factors $U_{kt}^{(\mathrm{CF+LP}),\theta}(clo)$:

	$E''\beta''$
ν_3	$34.640c_1-29.653$
ν_4	$22.775c_2+9.991$
ν_6	$-14.812c_2+19.662$

	U'_κ	U'_λ	U'_μ	U'_ν
ν_3	$19.280c_2-6.655$	$10.447c_2+11.279$	$26.114c_2-17.532$	0
ν_4	$6.760c_2+5.324$	$6.336c_2-7.204$	$14.437c_2-4.876$	0
ν_6	$-2.940c_2+5.573$	0	$-3.733c_2-13.997$	$-2.262c_2-10.262$

[1] P. A. Tanner, V. V. R. K. Kumar, C. K. Jayasankar, and M. F. Reid, J. Alloys Comp. **215**, 349 (1994).
[2] D. M. Moran, P. S. May, and F. S. Richardson, Chem. Phys. **186**, 77 (1994).
[3] T. R. Faulkner and F. S. Richardson, Mol. Phys. **36**, 193 (1978).
[4] P. A. Tanner and G. G. Siu, Mol. Phys. **75**, 233 (1992).
[5] T. R. Faulkner and F. S. Richardson, Mol. Phys. **35**, 1141 (1978).
[6] R. Acevedo, G. Díaz, and T. Meruane, Ann. Chem. **86**, 467 (1990).
[7] R. Acevedo and C. D. Flint, Mol. Phys. **56**, 683 (1985).
[8] R. Acevedo and C. D. Flint, Mol. Phys. **58**, 1033 (1986).
[9] J. P. Morley, T. R. Faulkner, F. S. Richardson, and R. W. Schwartz, J. Chem. Phys. **77**, 1710 (1982).
[10] R. W. Schwartz, T. R. Faulkner, and F. S. Richardson, Mol. Phys. **38**, 1767 (1979).
[11] O. L. Malta, J. Phys. Chem. Solids **56**, 1053 (1995).
[12] B. R. Judd, Phys. Scr. **21**, 543 (1979).
[13] R. A. Satten, C. L. Schreiber, and E. Y. Wong, J. Chem. Phys. **78**, 79 (1983).
[14] M. F. Reid and F. S. Richardson, Mol. Phys. **51**, 1077 (1984).
[15] G. Blasse, Int. Rev. Phys. Chem. **11**, 71 (1992).
[16] P. Caro, O. K. Moune, E. Antic-Fidancev, and M. Lemaitre-Blaise, J. Less Common Met. **112**, 153 (1985).
[17] G. Blasse, Top. Current Chem. **171**, 1 (1994).
[18] R. Acevedo, S. O. Vasqez, and C. D. Flint, Mol. Phys. **74**, 853 (1991).
[19] R. Acevedo and C. D. Flint, Mol. Phys. **58**, 1033 (1986).
[20] R. Acevedo, T. Meruane, E. Cortés, S. O. Vásquez, and C. D. Flint, Theor. Chim. Acta (Berl.) **88**, 99 (1994).
[21] M. Stavola and D. L. Dexter, Phys. Rev. B **20**, 1867 (1979).
[22] M. Stavola, J. Lumin. **31/32**, 45 (1984).
[23] M. Stavola, J. M. Friedman, R. A. Stepnoski, and M. G. Sceats, Chem. Phys. Lett. **80**, 192 (1981).
[24] M. Stavola, L. Isganitis, and M. G. Sceats, J. Chem. Phys. **74**, 4228 (1981).
[25] J. Dexpert-Ghys and F. Auzel, J. Chem. Phys. **80**, 4003 (1984).
[26] G. Blasse and L. H. Brixner, Inorg. Chim. Acta **169**, 25 (1991).
[27] G. P. Knudsen, F. W. Voss, R. Nevald, and H.-D. Amberger, in *Rare Earths in Modern Science and Technology*, edited by G. J. McCarthy, H. B. Silber, and J. J. Rhyne (Plenum, New York, 1982), Vol. 3.
[28] B. Bleaney, A. G. Stephen, P. J. Walker, and M. R. Wells, Proc. R. Soc. London Ser. A **381**, 1 (1982).
[29] M. R. Roser, J. Xu, S. J. White, and L. R. Corruccini, Phys. Rev. B **45**, 12 337 (1992).
[30] B. Kanellakopulos, H.-D. Amberger, G. G. Rosenbauer, and R. D. Fischer, J. Inorg. Nucl. Chem. **39**, 607 (1977).
[31] M. Bouazaoui, B. Jacquier, C. Linares, and W. Strek, J. Phys. C **3**, 921 (1991).
[32] C. J. Ballhausen, in *Vibronic Processes in Inorganic Chemistry*, edited by C. D. Flint (Kluwer, Netherlands, 1989), p. 53.
[33] A. A. Kaminskii, A. A. Kornienko, and M. I. Chertanov, Phys. Status Solidi B **134**, 717 (1986).
[34] G. Meyer, Prog. Solid State Chem. **14**, 141 (1982).
[35] W. Urland, Z. Naturforsch. Teil A **34**, 1507 (1979).
[36] E. Bucher, H. J. Guggenheim, K. Andres, G. W. Hull, and A. S. Cooper, Phys. Rev. B **10**, 2945 (1974).
[37] B. D. Dunlap, G. R. Davidson, M. Eibschutz, H. J. Giggenheim,

and R. C. Sherwood, Bull. Am. Phys. Soc. **19**, 369 (1974).
[38] R. Becker, A. Lentz, and W. Sawodny, Z. Anorg. Allg. Chem. **420**, 210 (1976).
[39] L. R. Morss, M. Siegal, L. Stenger, and N. Edelstein, Inorg. Chem. **9**, 1771 (1970).
[40] P. W. Atkins, *Physical Chemistry* (Oxford University Press, United Kingdom, 1978), p. 586.
[41] W. C. McCrone, L. B. McCrone, and J. G. Delly, *Polarized Light Microscopy*, 8th ed. (McCrone Research Institute, Chicago, 1985), p. 125.
[42] R. Acevedo, in *Vibronic Processes in Inorganic Chemistry, Advanced Study Institute, NATO Series C: Mathematical and Physical Sciences*, edited by C. D. Flint (Kluwer Academic, Dordrecht, 1989), pp. 139–194.
[43] A listing of these quantities is available from R. A.
[44] J. S. Griffith, *The Theory of Transition-Metal Ions* (Cambridge University Press, Cambridge, 1961).
[45] R. M. Golding, Mol. Phys. **21**, 157 (1971).
[46] P. N. Schatz, Spectrochim. Acta **21**, 617 (1965).
[47] S. Califano, *Vibrational States* (Wiley Interscience, New York, 1976).
[48] R. Acevedo, S. Vasquez, and M. Passman, An. Quim. **90**, 237 (1994).
[49] P. A. Tanner, Mol. Phys. **57**, 697 (1986).
[50] P. A. Tanner, Mol. Phys. **58**, 317 (1986).
[51] A. Barbanel, G. P. Chudnovskaya, I. Gavrish, R. B. Dushin, V. V. Kolin, and V. P. Kotlin, J. Radioanalyt. Nucl. Chem. **143**, 113 (1990).
[52] M. Choca, J. R. Ferraro, and K. Nakamoto, Coord. Chem. Rev. **12**, 295 (1974).
[53] P. A. Tanner and M.-Y. Shen, Spectrochim. Acta **50A**, 997 (1994).
[54] B. R. Judd, Phys. Rev. **127**, 750 (1962).
[55] G. S. Ofelt, J. Chem. Phys. **37**, 511 (1962).
[56] M. Galczynski and W. Strek, J. Phys. Chem. Solids **52**, 681 (1991).
[57] M. Galczynski and W. Strek, in *Proceedings of the 2nd International School on Excited States of Transition Elements*, Karpacz 1991, edited by W. Strek *et al.* (World Scientific, Singapore, 1992), p. 335.
[58] V. M. Orera, L. E. Trinkler, R. I. Merino, and A. Larrea, J. Phys. Condens. Matter **7**, 9657 (1995).
[59] T. Luxbacher, H. P. Fritzer, and C. D. Flint, Chem. Phys. Lett. **232**, 571 (1995).
[60] G. Blasse, A. Meijerink, and C. Donegá, J. Alloys Comp. **225**, 24 (1995).